Evaluation of Deoxidization Techniques during Vacuum Induction Melting of Titanium Alloys

B. Rotmann[1], H. Vogel[1], B. Friedrich[1]

[1]IME Process Metallurgy and Metal Recycling, RWTH Aachen University, Intzestrasse 3, 52062 Germany

Keywords: titanium, recycling, deoxidization, vacuum induction melting

Abstract

Despite their outstanding properties, titanium alloys still are mainly applied in fields where either no adequate substitution is available or the high material costs are subordinated to performance. This situation is the result of cost considerations: On the one hand, substitutes for the inefficient titanium production process (Kroll process) are not likely to be established within the next decade. On the other hand, recycling of titanium alloys focuses generally on selected and classified scrap, whereas the cheaper contaminated and inhomogeneous scrap is mostly downgraded to ferrotitanium. Therefore, utilization of the currently downgraded scrap fraction as feed stock material in a recycling process would result in new cost-competitive secondary titanium alloys. The processing route developed at IME consists of scrap pre-treatment, vacuum induction melting (VIM) in a high-purity calcia crucible and further refining by vacuum arc remelting (VAR). Contrary to conventional recycling routes, the introduction of the VIM step as new key feature allows the homogenization of the whole batch as well as supplementary metallurgical operations. However, with VIM of titanium alloys, two major challenges arise: Due to the high reactivity of titanium, VIM cannot be conducted in conventional ceramic crucibles – only less established materials such as CaO and Y_2O_3 exhibit sufficient thermodynamic stability towards titanium. On the other hand, oxygen pickup from the ceramic crucibles cannot be entirely inhibited. Therefore, a deoxidizing step is inevitable in order to compensate the additional oxygen. This research paper presents various deoxidization techniques during vacuum induction melting and assesses them by feasibility and efficiency. Furthermore, a test series is conducted in order to test the most promising approaches.

Introduction

Titanium and titanium alloys show a wide range of interesting properties, thus being a common choice in applications that benefit from their high strength at low density, high corrosion resistance and bio-compatibility. Nevertheless, with current titanium sponge prices of 11.38 $/kg [1], cost considerations still hinder its prevalence in mass applications. Unlike costs for other high-priced metals, titanium price levels are not justified by a raw material shortage but by an intricate production procedure, consisting of three main steps: titanium sponge production (Kroll process), remelting and further processing to semi-finished products and final components. However, substantial cost reductions can be achieved by recycling. Similar to aluminum recycling, the incentive for titanium recycling lies in the saving of a relatively high amount of energy that is needed to transfer the raw material into the metallic state. Thus, expenses related to the Kroll Process can be avoided. In addition, intensive machining, with buy-to-fly ratios as high as 20, leads to a substantial production of in-house revert, also referred to as new scrap. This provides the market with sufficient scrap capacities: In 2006, titanium ingot production accounted for a total of 145,000 t, thereof 35,000 t of scrap were recycled as feedstock material [2]. Clean and sorted scrap is usually introduced into the remelting step of the primary route: While lose scrap can be used for cold hearth melting without further preparation, vacuum arc remelting demands to mix the scrap with titanium sponge and to compress it to electrodes.

Nonetheless, conventional recycling routes exhibit a very limited refining potential with regard to oxygen contamination. Since e.g. turnings and chips display augmented oxygen levels caused by thick oxide layers and high surface-to-volume ratios, the potential feedstock share of scrap is narrowed in accordance with the desired maximum oxygen concentration. Another serious drawback is the small volume of the metal that is molten at one time during all titanium remelting processes except for the cost-intensive induction skull melting. This requires either mono-fraction feedstock or multiple remelting steps in order to achieve homogenous material. Therefore, only clean, classified in-house scrap is suitable for conventional recycling, leaving aside the dirty or mixed scrap shares. A market analysis in 2006 revealed that more than half of the available scrap is downgraded to master alloys like ferrotitanium and therefore permanently lost for the titanium cycle (Figure 1). It can be assumed that this share mainly consists of non-classified, highly contaminated turnings and scrap from used parts. While utilization of this cheaper scrap share as feedstock results in a substantial cost reduction, the conventional recycling process doesn’t qualify for this share due to restrictions regarding refining and homogenization.

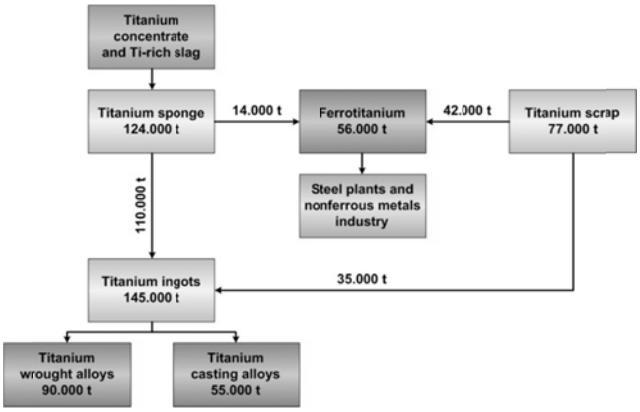

Figure 1:Flow chart of titanium production [2]

As shown in Figure 2, the titanium recycling process developed at IME consists of three main steps: Conditioning, vacuum induction melting and vacuum arc remelting. The process route is designed to handle scrap from various sources including up to 100 % low-grade scrap turnings, being the worst case scenario regarding contamination and processing behavior. Other scrap qualities can easily be introduced into the process at a later point in time, e.g. clean scrap turnings after washing or bulk scrap after briquetting. Hence, the proposed process allows considerable cost benefits that could support the market entry for titanium in mass applications.

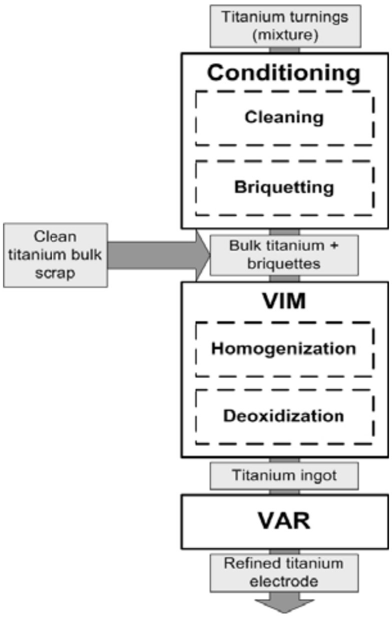

Figure 2: IME Recycling Process flowchart

The main goals of conditioning (step 1) are reducing impurities that come along with the scrap as well as compacting of lose scrap. As a first step of the conditioning, drying of the turnings is performed at 120 °C for evaporation of water, which is a major component of commercially used lubricants. Afterwards, the turnings are cleaned with ethanol in order to remove remaining oil-based lubricants and then dried again. Subsequently, the turnings are mixed and pressed to compacts in order to ensure satisfactory energy input during vacuum induction melting. As final conditioning step, the briquettes are heated up to 400 °C to assure the removal of remaining organic compounds. Bulk scrap can be spared from this procedure, since it is already compact enough for inductive coupling and it generally shows sufficient surface cleanness.

In the IME Recycling Process vacuum induction melting (step 2) is carried out in order to melt down the batch and to achieve a homogenous composition in one single process step. Despite its advantages, VIM has not been applied to titanium remelting so far. This is due to the lacking stability of conventional refractories towards titanium. According to the Ellingham diagram (Figure 3), only a few oxide-based ceramics exhibit sufficient thermochemical stability above the melting temperature of titanium, including CaO, ZrO_2 and Y_2O_3. While only CaO and Y_2O_3 proved to be stable towards Ti-6Al-4V in a lab scale test, CaO was chosen as crucible material based on cost considerations. Nevertheless, the advantages of VIM come at the expense of increased oxygen levels due to the decomposition of the CaO crucible, which leads to a rise of the oxygen concentration in the melt.

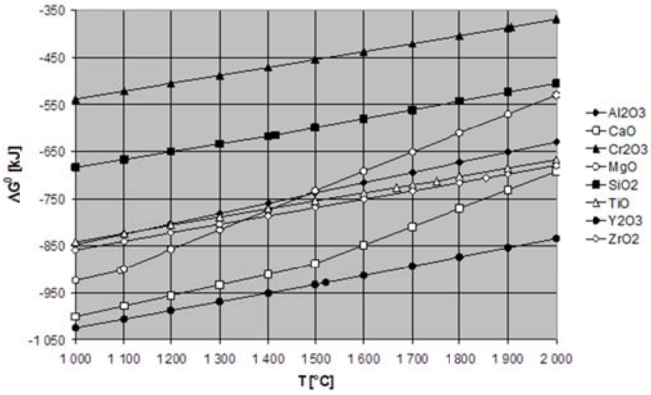

Figure 3: Standard Gibbs energies of formation $\Delta G^0(T)$ of crucible oxides versus titanium (+II) oxide (FactSage 5.4.1, Data: SGPS)

The final vacuum arc remelting (step 3) is carried out in order to reduce volatile elements, such as calcium, to remove non-metallic inclusions and to ensure the desired grain structure and orientation. To counteract the oxygen pickup, a deoxidizing process is mandatory and remains the key challenge in order to ensure the success of the proposed alternative recycling concept.

Fundamentals

As pointed out in the previous chapter, the ceramic CaO crucible decomposes during melting until the thermodynamic equilibrium is reached. Consequently, the crucible wears off and the oxygen concentration in the melt rises. Beyond that, the initial oxygen contamination of the scrap feedstock generally exceeds the accepted levels according to the applying specifications. As an interstitial element, oxygen causes embrittlement of the titanium alloy [3]. Without deoxidization treatment, the ingot after VIM can be so brittle that it does not even withstand the thermally induced mechanical strains and cracks into pieces. Hence, the decomposition reaction is examined for the purpose of a quantitative assessment:

$$< CaO > \rightarrow [Ca]_{Ti} + [O]_{Ti} \qquad (1)$$

<CaO>: calcium oxide, solid; $[Ca]_{Ti}$: calcium, dissolved in titanium, $[O]_{Ti}$: oxygen, dissolved in titanium

In this context, the equilibrium constant K is calculated according to the law of mass action. K is described as follows:

$$K = \frac{f_{Ca}\cdot[wt.-\%\,Ca]\cdot f_O\cdot[wt.-\%\,O]}{a_{CaO}} \qquad (2)$$

a_{CaO}: activity of CaO; f_{Ca}, f_O: activity coefficients of Ca and O; $[wt.-\%\,Ca], [wt.-\%\,O]$: Ca- and O-concentration in liquid titanium

In order to determine the equilibrium conditions, it is necessary to calculate the activity coefficients. The activity of calcium oxide equals one, as the melt is in constant contact to the calcium oxide crucible. The activity coefficients of calcium and oxygen cannot be easily determined. However, the first-order interaction parameter can be used as approximation [4]:

$$\log f_{Ca} = e_{Ca}^{Ca}\ [wt.-\%\,Ca] + e_{Ca}^{O}[wt.-\%\,O] \qquad (3)$$

$$\log f_O = e_O^{Ca}\ [wt.-\%\,Ca] + e_O^{O}\ [wt.-\%\,O] \qquad (4)$$

e_Y^X: interaction parameter

Here, the self-interaction coefficient e_O^O and e_{Ca}^{Ca} will not be considered due to their negligible low values. With the interrelation between the interaction parameter and the molar masses of calcium and oxygen (M_o, M_{ca}) [4]

$$e_O^{Ca} = e_{Ca}^{O}\cdot\left(\frac{M_O}{M_{Ca}}\right) \qquad (5)$$

the following relation is the result of adopting the equations of the interaction parameter in equation 2 [4]:

$$\log\ [wt.-\%\,Ca]\cdot[wt.-\%\,O] = \log K - e_{Ca}^{O}\left([wt.-\%\,O] + \left(\frac{M_O}{M_{Ca}}\right)\cdot[wt.-\%\,Ca]\right) \qquad (6)$$

Tsukihashi et al. determined values for the concentration of calcium and oxygen in equilibrium with solid calcium oxide at 1730 °C on the basis of experimental data [4]. Under these conditions, the logarithm of the equilibrium parameter can be determined. The result is the value log K = -1.75 and an interaction parameter of e_{Ca}^{O}= -0.019. Based on the value for 1730 °C, Lochbichler approximates the solubility product starting from 1750 °C up to 1550 °C [5]. The graphical result for the resulting saturation concentrations of oxygen and calcium in equilibrium with solid calcium oxide in liquid titanium are displayed in Figure 4.

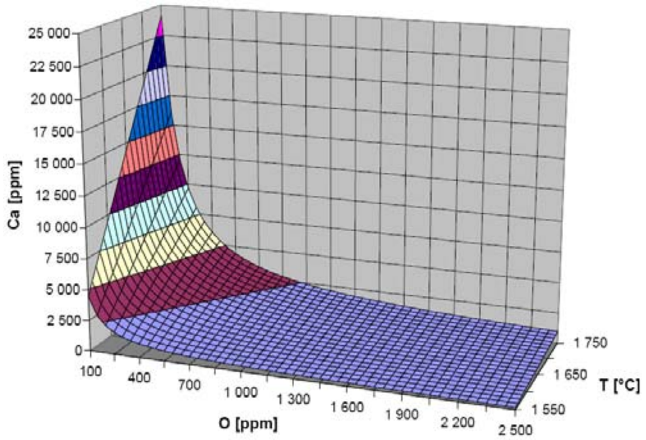

Figure 4: Temperature-dependent saturation concentration (mass ppm) of calcium and oxygen in TiAl50/Ti in contact with CaO [5]

This concentration curve clearly shows that a deoxidization at a thermodynamic equilibrium is only successful with a stabilization of the melt with calcium.

As pure calcium has a boiling point of 1484 °C [6], an excessive mass loss related to evaporation can be expected: According to [7], the partial pressure of pure calcium can be described as:

$$\ln p_{Ca} = 25.7691 - 20283.9\,T^{-1} - 1.0216\,\ln T \qquad (7)$$

p_{Ca}: partial pressure of pure calcium [Torr], T: temperature [K]

At a process temperature of 1700°C, this returns a partial pressure of 3.05 bar. Hence, in progress of the melting time, the calcium concentration declines, while the oxygen concentration rises according to the thermochemical equilibrium. As a result, calcium should either be feeded continuously in order to cover the losses or holding time after deoxidization has to be kept as short as possible. The latter option is difficult, since a certain period of time is usually intended to allow full homogenization of the melt after the deoxidization treatment.

In summary, the following preconditions have to be fulfilled for a successful and effective deoxidization:

- Saturation of the melt with calcium
- Identification of a suitable deoxidization agent
- Diminishment of calcium losses
- Continuous feeding of calcium, if possible

As the saturation of the melt with calcium has already been discussed, the next step is the identification of a deoxidization agent. The reaction can be described as follows:

$$y[TiO]_{Ti} + x[Me]_{Ti} = < Me_xO_y > + y[Ti]_{Ti} \qquad (8)$$

Me: deoxidization element

The standard formation enthalpies of Y_2O_3, CaO and ZrO_2 are below the TiO-value for process temperatures around 1720 °C (Figure 3). These oxides are more stable than TiO, whereas the enthalpy value for the creation of ZrO_2 is right below the TiO-value. Hence, a sufficient deoxidization effect is not given for zirconium. Consequently, the remaining materials for a successful deoxidization of titanium are calcium and yttrium. As calcium has already been added in order to prevent the melt from further oxygen pickup from crucible decomposition, it is a natural choice as deoxidization agent. Besides, in contrast to yttrium, calcium is easily removed via distillation during the VAR (step 3), therefore avoiding a contamination of the final alloy with the deoxidization agent. Moreover, the deoxidization product CaO is floated to the surface, while Y_2O_3 remains in the melt. As a final point, calcium is less expensive than yttrium. In order to minimize calcium losses, different concepts can be applied:

First of all, process pressure can be increased. According to equation 7, by setting up a process pressure beyond 3.05 bar, boiling of the melt can be inhibited. This measure is not only beneficial for process handling but also contributes to the reduction of evaporation losses. However, significant decrease of evaporation has only been reported at pressures above 20 bar – a value that technical-scale vacuum induction furnaces cannot sustain (yet).

Another possibility to optimize the process is the reduction of calcium's vapor pressure. This can be achieved by adding calcium in form of a master alloy into the melt. In that context, intermetallic phases are suitable in particular, as they are characterized by high melting points if the ratio of ingredients results in a congruent melting phase. Consequently, these phases have a lower vapor pressure as pure calcium. Applicable samples for intermetallic phases with calcium are calcium-silicon or calcium-aluminum. While CaSi is a very common alloy for deoxidization and desulphurization of steel melts, [8], CaAl alloys are more suitable in the present work due to the following reason: Al is an alloying element in numerous titanium alloys with contents up to 6 wt.-%, whereas Si is rarely used and generally limited to approximately 0.35 wt.-%. [9] Therefore, by utilization of a CaSi alloy, only massive diluting via adding virgin titanium sponge will bring the final alloy within the reach of common titanium specifications. Vapor pressures of calcium above calcium-aluminum and calcium-silicon melts can be calculated according to the following equation for different temperatures [10]

$$\ln p_{Ca} = \frac{-18482 + {}^{\Delta H_{Ca,X}}/_{R}}{T} + 17{,}111 + \ln x_{Ca} - {}^{\Delta S^{E}_{Ca,X}}/_{R} \qquad (9)$$

With experiment-based values for the partial enthalpy of mixing, the corresponding values can be included together with R (general gas constant) in the formula. As an example, the mixing enthalpy for the calcium-aluminum melt is $\Delta H_{Ca,0,3}$= -6902.8 whereas the partial excess entropy is $\Delta S^{E}_{Ca,0,3}$= -1.337 for a mole fraction of calcium of $x_{Ca(Ca-Al)}$ = 0.3. Consequently, the vapor pressures p_{Ca} can be calculated. Figure 5 displays the vapor pressures of two different mole fractions of calcium (0.3 and 0.7) over a liquid 2-phase-mixture of calcium-aluminum.

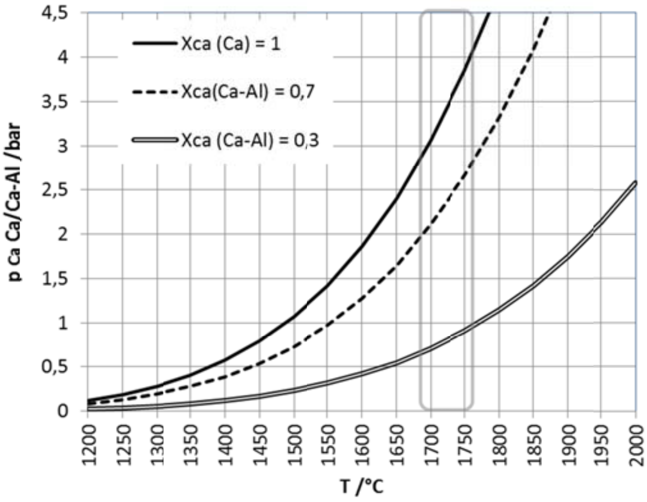

Figure 5: Calcium vapor pressure over a pure calcium and calcium-aluminum melt, Note: the area of the process temperature is framed in grey. . (Data: [10])

The utilization of a $CaAl_2$-alloy instead of elemental Ca has further advantages: The melting point of $CaAl_2$ is significantly higher than that of pure calcium (1079 °C versus 842 °C, [11]) and therefore delays melting down of the deoxidizing agent when dipped into the melt. Consequently, $CaAl_2$ can be introduced into the melt instead of floating on the melt, subsequently reacting to calcium in dissolved and gaseous state: Formation of calcium gas bubbles may occur, which can also react with the dissolved oxygen.

$$< CaAl_2 > = [Ca]_{Ti} + 2[Al]_{Ti} \qquad (10)$$

$$[Ca]_{Ti} = \{Ca\} \qquad (11)$$

Afterwards, calcium reacts with the dissolved oxygen, forming CaO:

$$[TiO]_{Ti} + [Ca]_{Ti} = < CaO > + [Ti]_{Ti} \qquad (12)$$

$$[TiO]_{Ti} + \{Ca\} = < CaO > + [Ti]_{Ti} \qquad (13)$$

Due to the lower density of CaO compared to the melt and the intense stirring during VIM, the oxide particles are floated to the surface. Following the melt flow, they are transported to the edge, where they can cluster at the refractory walls. Based on these results, this paper's experiments include an immersion deoxidization with $CaAl_2$.

Concerning the continuous feeding of the deoxidization agent, different options seem possible: A first possible approach is the introduction of gaseous calcium via an injector, porous plug or a conventional gas purging lance. The design requirements of such a system are comparatively sophisticated and therefore costly, high calcium losses can be expected, and the impact of additional security measures cannot be neglected. However, such a setup would allow excellent process control, as the mass flow could be adjusted to exactly level the evaporation losses. Moreover, casting could be conducted immediately after the end of deoxidization, since no extra compounds such as aluminum have to be homogenized within the melt.

Alternatively a high melting, high density alloy, consisting of calcium, common titanium alloying elements and/or volatile elements could be introduced into the melt. The melting point should be around 1700 °C and the density should preferably exceed 6 kg/m³. Such an alloy would presumably sink to the bottom, slowly dissolve and therefore give a continuous deoxidization treatment. However, in praxis no such alloy could be identified.

Limited by the available means in laboratory scale, a compromise is found. A mixture of CaO and $CaAl_2$ is compacted to pellets and introduced to the melt. Although the lower density in comparison to the melt should result in floating on the melt, the pellet should first harden due to sintering, than slowly dissolve due to the large fraction of high-melting CaO, freeing the entrapped $CaAl_2$ and therefore resulting in a continuous deoxidization process.

A second, completely different approach is the utilization of an active slag. Although the concept is proved to work in an electroslag remelting (ESR) process (see [12] for further information), entirely different circumstances lead to a number of necessary additional considerations. In order to prohibit the destruction of the CaO crucible, the slag has to be basic. Further, formation of low-melting mixtures with CaO should be avoided. The activity of calcium has to be high enough to allow the reaction of calcium with the oxygen within the melt. In order to enhance the reaction between slag and metal, the melting point of the slag should be at least 100 °C below the process temperature. Oxidic slag components have to be thermodynamically more stable than TiO to ensure the deoxidization of titanium instead of the slag components by calcium. Another challenge is the phase separation of slag and metal after the conducted deoxidization. This challenge displays a further research area and is not further considered in this research paper. However, a decantation while casting or bottom tapping seems possible.

The slag CaO-CaF_2-Ca, which is used during the ESR-approach at least partially fulfills these conditions. CaO as basic component would even stabilize the crucible as the liquid CaO from the slag should easier dissolve than the CaO from the crucible. However, CaO has a melting point of 2613 °C, leading to a necessary addition of a flux to produce a flowable slag. Hence, the addition of CaF_2 is unavoidable. As CaO and CaF_2 are entirely mixable, a CaO-saturation within the CaF_2 cannot be achieved and the reaction with the crucible cannot be prevented completely. A deoxidization with the help of a slag on the basis of the components CaO and CaF_2 can only succeed if the reaction with the CaO crucible is sufficiently kinetically inhibited to survive a minimum number of melts without damage.

Another possibility is to find a slag system that is not based on CaO. However, this system has to be basic as well. Simultaneously, this system has to provide Ca. The identified potential oxides, e.g. MgO, exhibit similar chemical behavior as CaO - an appropriate flux for this compound would also dissolve the CaO-crucible upon contact. Instead, low-melting, basic oxides, such as Li_2O, could be an option. However, there exists no low-melting oxide which is more stable than TiO. That means that with the addition of calcium, metallic lithium would be produced, instead of a deoxidization of titanium.

The resistance of a CaO crucible towards a CaO-CaF_2-based slag is therefore examined in a preliminary lab-scale test.

Experimental Investigation

Based on the theoretical considerations, three different experimental setups are arranged in order to test the general feasibility of these approaches:

- Active slag deoxidization
- CaO-$CaAl_2$ pellet deoxidization
- Immersion deoxidization

In order to enhance crucible lifetime, TiAl alloys are used instead of c.p. titanium.

Active slag deoxidization

The first preliminary test is conducted in order to evaluate the stability of a self-made CaO crucible towards a CaO-CaF_2-$CaAl_2$-based slag. Although the CaF_2 component should react with the crucible, the reaction might be kinetically limited, allowing enough time to carry out the process.

The slag consists of 57,5 wt.-% CaF_2, 22,5 wt.-% CaO and 20 wt.-% $CaAl_2$. Overall, 12.7 g of slag are mixed and put into the CaO crucible, which has a total length of 80 mm and an inner diameter of 20 mm. The crucible is placed in a graphite susceptor (figure 6), the furnace is evacuated and set to an atmosphere of 600 mbar argon.

Figure 6: Furnace setup with graphite susceptor

Following, the mixture is heated with a power input of 2 kW. At around 1000 °C, the first formation of smoke can be observed; power is increased to 5 kW. At 1423 °C, the slag changes into liquid state - shortly after, the first bubbles can be noticed. Slag agitation and formation of bubbles intensify with rising temperature and come to a maximum at around 1600 °C. Both thermocouples fail afterwards, the trial is continued until a total holding time of liquid slag of 35 minutes is reached. The temperature at the end is estimated to be around 1700 °C.

CaO-CaAl$_2$ pellet deoxidization

The second experiment comprises the fabrication of two CaO-CaAl$_2$ pellets and their melting together with TiAl in two high-purity Al$_2$O$_3$ crucibles. CaAl$_2$ is mixed together with CaO in a ratio of 1:2 and compacted to pellets with a pressure of 125 MPa. While pellet C features a CaAl$_2$ grain size between 0.6 mm and 1.5 mm, the grain size of pellet D is between 1,5 and 5 mm (figure 7).

Figure 7: Pellet C

According to theoretical considerations, the Al$_2$O$_3$ crucible offers only limited stability towards TiAl melts. However, it is considered to be sufficient for a single trial. Moreover, the distinction between crucible material and CaO from the pellet is significantly improved.

The first crucible is filled with 71.1 g of TiAl40 alloy (see table 1) and pellet C pieces with a total mass of 11.3 g, while the second charge consists of 74.3 g of TiAl40 alloy and pellet D pieces with a total mass of 36.6 g. The crucibles are put in the graphite susceptor from figure 6, the vacuum induction furnace is evacuated and an argon pressure of 500 mbar is adjusted. Power input is gradually increased - after 50 minutes and at a temperature of 1160 °C all pellets emit smoke. At 1490 °C, the TiAl seems to soften, while the pressure increases to 550 mbar. The metal melts at 1510 °C and shortly after, the pellet starts to dissolute. Starting from 1550 °C, formation of bubbles and intense agitation of the molten bath is observed. The pressure in the furnace rises to 600 mbar and vision is considerably impaired. After 10 minutes of contact between the melt and the pellets, the power is switched off and the melt solidifies in the crucibles.

Immersion deoxidization

The last experiment is conducted in order to evaluate the potential of immersion deoxidization. For this purpose, a can made of low-carbon steel serves as container for the CaAl$_2$ grains. Although potentially following trials should be carried out with a titanium can, no impact on the results other than introduction of iron and carbon to the alloy is expected due to the utilization of steel. The can has a diameter and height of 40 mm and a wall thickness of 1 mm (figure 8). It is perforated to allow instant contact between melt and deoxidization agent, while pushing the container below the melt surface. The can is filled with 32.7 g CaAl$_2$ with a grain size between 1.5 and 5 mm.

Figure 8: Deoxidization can; left: filled with $CaAl_2$ granules, right: with lid

The experiment is conducted in a commercially available CaO crucible with an inner diameter of 100 mm and a wall thickness of 10 mm, the maximum capacity is 2.5 dm^3. The crucible is charged with 1800g TiAl37 (table 2), before the furnace is flooded with argon and subsequently evacuated to a pressure of $2 \cdot 10^{-2}$ mbar. Following, a moderate input power of 4 kW is applied in order to avoid fast heating and thermally induced strains. After 40 minutes and at a temperature of 1200 °C, the power is increased to 6 kW. 20 minutes later, the temperature has reached 1560 °C and the furnace atmosphere is now adjusted to 700 mbar. The first melt is visible and the power is further increased. Five minutes later, the whole batch is molten, while the furnace atmosphere has risen to 745 mbar. The deoxidization procedure is started after a total time span of 90 minutes: the vacuum lock above the crucible is opened and the deoxidization can is pushed to the bottom of the crucible. After 8 seconds, smoke emission starts and stays massive for 30 seconds. Afterwards, smoke emission decreases, the vision is reestablished after 60 seconds. The melt appears to be turbulent, but bubble formation cannot be detected. Directly after deoxidization, a solid layer can be observed on the surface (figure 9), which is floated to the edge and disappears after some minutes. The input power is again increased to 8 kW in order to allow superheating of the melt for casting, which takes place 5 minutes and 30 seconds after the deoxidization.

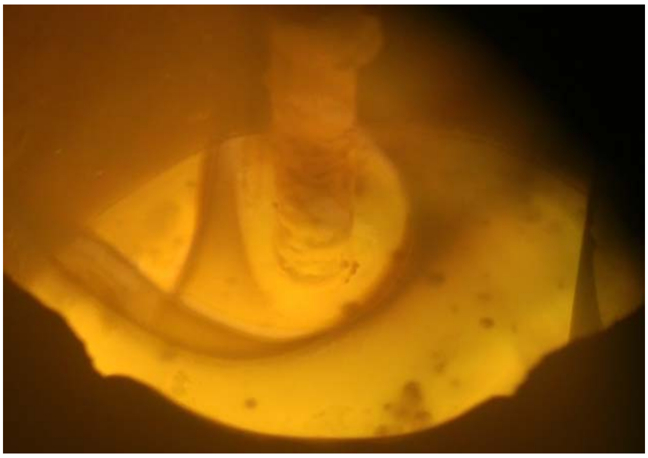

Figure 9: Solid layer floating on the melt after deoxidization treatment

Experimental Results

Active slag deoxidization

As can be seen in figure 10, the CaF_2-based slag leads to massive crucible infiltration and dissolution. Unfortunately, no kinetic limitation was found to significantly inhibit the reaction between CaF_2 from the slag and the CaO crucible. Even though the attack might be less severe in more dense commercially available crucibles, the results of this test lead to the assumption, that CaF_2-based slags are not suitable for deoxidization in CaO crucibles. Therefore, further trials have not been conducted.

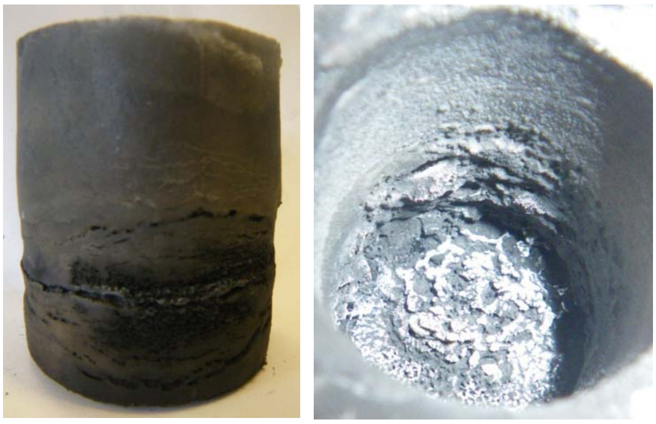

Figure 10: CaO crucible after slag treatment; left: soaked crucible, right: massive reaction between slag and crucible on the inner layer

CaO-$CaAl_2$ pellet deoxidization

No impact of either $CaAl_2$ grain size or total pellet mass could be observed. Concerning the deoxidization efficiency, only marginal oxygen pickup from the crucible can be noted (table 1).

composition	Al / wt.-%	Ca / wt.-%	O / ppm
initial	39.8	0.012	2800
with pellet C	38.4	2.67	3010
with pellet D	40.6	3.30	2855

Table 1: Composition of TiAl alloy before and after pellet C/D deoxidization, Ti wt.-% = balance

Moreover, extremely high calcium concentrations up to 33000 ppm have been found in the metal phase, which is a pre-condition for deep-deoxidization. However, the oxygen concentrations do not match the expected values from the solubility product: Giving the calculated solubility product of calcium and oxygen from figure 4, the oxygen content should stay below 100 ppm. This strongly indicates that equilibrium hasn't been reached in the conducted trial. However, according to figure 11, metal and the CaO phase exhibit excellent phase separation. Hence, deoxidization via addition of CaO-$CaAl_2$ pellets is possible.

Figure 11: Phase separation between metal and CaO

Immersion deoxidization

The chemical analysis of the resulting alloy is given in table 2: While changes in titanium and aluminum concentration are not beyond statistical significance, calcium and oxygen concentrations are elevated. However, the addition of the deoxidization agent corresponds to a rise of 7700 ppm calcium in the melt. With the formation of calcium oxide, the equilibrium should level off at 7077 ppm calcium and 57 ppm oxygen. According to the analysis, the calcium concentration is just 1200 ppm, which is supposedly caused by the observed massive evaporation during melting. The actual oxygen concentration in turn is not in accordance with the thermochemical equilibrium (333 ppm), but then again, the increase is moderate and still within the specification limits of TiAl alloys. Overall, satisfactory results have been obtained by immersion deoxidization.

composition	Ti / wt.-%	Al / wt.-%	Ca / ppm	O / ppm
initial	62.9	36.71	-	512
final	59.7	34.50	1200	960

Table 2: Composition of TiAl alloy before and after immersion deoxidization

Conclusion

The IME Recycling Process is a promising approach, which could lead to considerable cost reductions through the utilization of low-grade scrap as feedstock. However, with the implementation of VIM as a key feature of the process route, deoxidization becomes mandatory. The theoretical considerations confirm the feasibility of such a step during VIM. Nonetheless, the volatility of the most promising deoxidization agent, calcium, demands studies about the best practical implementation. The proposed active slag treatment seems to be not feasible due to the lack of a flux agent that is inert towards the crucible while forming a low melting slag with CaO and Ca. The deoxidization with CaO-$CaAl_2$ pellets shows promising results, although the existence of a second phase beside the metal phase could lead to issues like non-metallic inclusions.

Anyhow, the immersion deoxidization is by far the most promising approach: Oxygen pickup from the crucible decomposition is limited to acceptable levels and the implementation of the process can be done at justifiable efforts. However, an instant consumption of the entire deoxidization agent results in massive evaporation of calcium, which leads to an insufficient final calcium concentration in the melt and restricted vision in the furnace. Significant improvements of this matter could be drawn by implementing injection of cored wire, as known from steel deoxidization: First, the holding time for homogenization after the treatment could be kept to minimum, therefore limiting the calcium losses in the melt. Second, the continuous feeding of deoxidization agent would enable superior process control: Via spooling velocity, calcium input could be adjusted to compensate exactly for evaporation losses. Even the application of pure calcium as deoxidization agent is conceivable, eliminating the need for diluting with titanium sponge due to the aluminum input. The theoretical considerations and the results from the preliminary tests in the present work suggest the implementation of a deoxidization step via cored wire injection in order to enable the VIM of titanium. This will be validated in a technical-scale setup to gain more thorough understanding of the achievable efficiency.

References

[1] USGS: Mineral Commodity Summaries (2011); United States Geological Survey; Reston; VA; USA; page 172-173

[2] Angerer, G.; Erdmann, L.; Marscheider-Weidemann, F.; Scharp, M.; Lüllmann, A.; Handke, V.; Marwede, M. (2009); Rohstoffe für Zukunftstechnologien. Einfluss des branchenspezifischen Rohstoffbedarfs in rohstoffintensiven Zukunftstechnologien auf die zukünftige Rohstoffnachfrage; 2., überarb. Aufl.; Hg. v. Fraunhofer ISI. Karlsruhe; page 265

[3] Donachie, M. J. (2000); Titanium. A technical guide; 2nd. ed.; Materials Park, OH; ASM International; page 14

[4] Tsukihashi, F.; Hatta, T.; Tawara, E. (1996): Thermodynamics of calcium and oxygen in moltentitanium and titanium-aluminum alloy. In: Metall and Materi Trans B 27 (6); page 967–972.

[5] Lochbichler, C. S. (2011); Design eines prozessstufenarmen Titanrecyclingprozesses; Dissertation; IME Metallurgische Prozesstechnik und Metallrecycling, RWTH Aachen; page 56

[6] Smithells, C. J.; Gale, W. F.; Totemeier, T. C. (2004); Smithells metals reference book. 8th ed.; Amsterdam, Boston; Elsevier Butterworth-Heinemann; page 14.1

[7] Köhler, M., Engell, H.-J. , Janke, D. (1985); Excess pressure refining of steel melts using metallic calcium; In: Proceedings 8th International Conference Vacuum Metallurgy; Linz/Austria, Eisenhütte Österreich; page 851-68.

[8] Dyudkin, D. A.; Kisilenko, V. V. (2007); Modern technology for treating steel outside the furnace with cored wire. In: Metallurgist 51 3-4; page 165-171.

[9] Leyens, C.; Peters, M. (2002); Titan und Titanlegierungen, 3. Auflage. Weinheim

[10] Schürmann, E.; et al.(1975); Dampfdruck des Calciums über Calcium-Silicium- und Calcium-Aluminium-Schmelzen sowie über Calcium-Aluminium-Silicium-Legierungen. In: Archiv Eisenhüttenwesen 46; page 473–76.

[11] Predel, B.; in: Landolt-Börnstein - Group IV; Vol. 5, Springer-Verlag Heidelberg

[12] Stoephasius, J.-C. (2006); Elektroschlackeraffination aluminothermisch hergestellter γ-Titanaluminide; Dissertation; IME - Institut für Metallurgische Prozesstechnik und Metallrecycling; RWTH Aachen